Cross-Linking and Lipid Efflux Properties of ApoA-I Mutants Suggest Direct Association between ApoA-I Helices and ABCA1†

Angeliki Chroni,‡ Tong Liu,‡ Michael L. Fitzgerald,§ Mason W. Freeman,§ and Vassilis I. Zannis*,‡

Molecular Genetics, Whitaker Cardiovascular Institute, Departments of Medicine and Biochemistry, Boston University School of Medicine, 715 Albany Street W509, Boston, Massachusetts 02118, and Lipid Metabolism Unit, Massachusetts General Hospital and Harvard Medical School, Boston, Massachusetts 02114

Received October 7, 2003; Revised Manuscript Received December 9, 2003

ABSTRACT: To explore the functional interactions between apoA-I and ABCA1, we correlated the cross-linking properties of several apoA-I mutants with their ability to promote cholesterol efflux. In a competitive cross-linking assay, amino-terminal deletion and double amino- and carboxy-terminal deletion mutants of apoA-I competed effectively the cross-linking of WT ^{125}I-apoA-I to ABCA1, while the carboxy-terminal deletion mutant apoA-I[Δ(220−243)] competed poorly. Direct cross-linking of WT apoA-I, amino-terminal, and double deletion mutants of apoA-I to ABCA1 showed similar apparent K_d values (49−74 nM), whereas the apparent K_d values of the carboxy-terminal deletion mutants apoA-I[Δ(185−243)] and apoA-I[Δ-(220−243)] were increased 3-fold. Analysis of several internal deletions and point mutants of apoA-I showed that apoA-I[Δ(61−78)], apoA-I[Δ(89−99)], apoA-I[Δ(136−143)], apoA-I[Δ(144−165)], apoA-I[D102A/D103A], apoA-I[E125K/E128K/K133E/E139K], apoA-I[L141R], apoA-I[R160V/H162A], and WT apoA-I had similar ABCA1-mediated lipid efflux, and all competed efficiently the cross-linking of WT ^{125}I-apoA-I to ABCA1. WT apoA-I and ABCA1 could be cross-linked with a 3 Å cross-linker. The WT apoA-I, amino, carboxy and double deletion mutants of apoA-I showed differences in the cross-linking to WT ABCA1 and the mutant ABCA1[W590S]. The findings are consistent with a direct association of different combinations of apoA-I helices with a complementary ABCA1 domain. Mutations that alter ABCA1/apoA-I association affect cholesterol efflux and inhibit biogenesis of HDL.

ApoA-I[1] is the major protein constituent of HDL and plays a pivotal role in the metabolism and function of HDL (*1*). ApoA-I can induce cholesterol efflux from cells, a process that is crucial for regulating cellular free cholesterol homeostasis (*2*), receptor endocytosis and recycling (*3*), and cell signaling (*4*). Lipid-free apoA-I can promote efflux of cellular phospholipids and cholesterol by an ATP-dependent process, which involves the ABCA1 (*5*−*8*). The interaction of apoA-I with the ABCA1 results in the lipidation of apoA-I and formation of pre*β* HDL, discoidal HDL, and, after cholesterol esterification by LCAT, spherical α-HDL particles (*5*, *9*−*17*).

The mechanism of the functional interactions between ABCA1 and apoA-I is not fully resolved. Some investigators propose that the cholesterol acceptor does not interact physically with ABCA1 but rather that it binds to cell membrane domains in the vicinity of ABCA1 (*12*, *18*, *19*). Recently, analysis of the properties of ABCA1 mutants indicated that direct binding of apoA-I to ABCA1 is necessary but not sufficient to promote cholesterol efflux (*20*).

In a previous study (*21*), we found that the ABCA1-dependent lipid efflux was reduced greatly by carboxy-terminal deletions of apoA-I that remove the 220−231 region, was reduced slightly by amino-terminal deletions, and was restored to 75−80% of the WT apoA-I control value by double amino- and carboxy-terminal deletions.

To further examine the structural domains of apoA-I that affect the apoA-I/ABCA1 interactions, we tested the effect of amino-terminal, carboxy-terminal, and internal deletion mutants, as well as point mutants in the central helices of apoA-I on ABCA1-mediated lipid efflux and on the ability of apoA-I to cross-link to ABCA1. Furthermore, we tested the ability of apoA-I mutants to associate with the ABCA1[W590S] mutant, which is defective in cholesterol efflux but cross-links to apoA-I (*20*). We have found that there is a correlation between cross-linking of apoA-I to WT ABCA1 and lipid efflux in all of the apoA-I mutants. Cross-linking indicated that the reactive amino acids of apoA-I and ABCA1 are within a distance of 3 Å. The efflux capacity of apoA-I was maintained when the individual central helices were mutated, suggesting that combinations of different amphipathic helices of apoA-I can promote efflux with similar efficiency. The cross-linking ability of amino- and carboxy-terminal mutants to the WT and the mutant ABCA1 form was different. Taken together with other data, these

† This work was supported by National Institutes of Health Grants HL-48739 and HL-68988.

* To whom correspondence should be addressed. Tel: 617-638-5085. Fax: 617-638-5141. E-mail: vzannis@bu.edu.

‡ Boston University School of Medicine.

§ Massachusetts General Hospital and Harvard Medical School.

[1] Abbreviations: ABCA1, ATP binding cassette transporter A1; apoA-I, apolipoprotein A-I; BSA, bovine serum albumin; cpt-cAMP, 8-(4-chlorophenylthio)adenosine 3′:5′-cyclic monophosphate; DFDNB, 1,5-difluoro-2,4-dinitrobenzene; DSG, disuccinimidyl glutarate; DSP, dithiobis(succinimidylpropionate); FBS, fetal bovine serum; HDL, high-density lipoproteins; HEK293 cells, human embryonic kidney 293 cells; LCAT, lecithin:cholesterol acyltransferase; rTEV protease, recombinant tobacco etched viral protease; SR-BI, scavenger receptor class B type I; WT, wild-type.

10.1021/bi035813p CCC: $27.50
Published on Web 01/27/2004

Table 1: Oligonucleotides Used in PCR Amplification and Mutagenesis

name	sequence	location and other features
AIWC-5	5′-ACT CAA **GGA TCC**[a] GAT GAA CCC CCC CAG AGC CCC TGG GAT-3′	ACTCAA + *Bam*HI site followed by nt[b] 73−99 (sense) (amino acids +1 to +9)[c]
AIWC-3	5′-ACT CAA **GTC GAC** TTT TTC CCA CTT TGG AAA CGT TTA TTC TGA GCA-3′	ACTCAA + *Sal*I site followed by nt 864−832 (antisense) (poly A region)
AIMII1−5	5′-ATC GCA **GGA TCC** GAT GAA CCC CCC CAG AGC CCC TGG GAT CGA-3′	ATCGCA + *Bam*HI site followed by nt 73−102 (sense) (amino acids +1 to +10)
AIMII1−3	5′-ATT CTG **CCT CAG G**CC CTC TGT ... ...[d] CAG CTT GCT GAA G-3′	ATT + nt 324−307 including *Bsu36I* site followed by nt 252−240 (antisense) (amino acids +84 to +79 and amino acids +57 to +60)
AIMIII1−5	5′-CAG GAG ATG AGC AAG ... ... TAC CTG GAC GAC TTC-3′	nt 322−336 + nt 370−384 (sense) (amino acids +84 to +88 and amino acids +100 to +104)
AIMIII1−3	5′-GAA GTC GTC CAG GTA ... ... CTT GCT CAT CTC CTG-3′	nt 384−370 + nt 336−322 (antisense) (amino acids +104 to +100 and amino acids +88 to +84)
AI*Not*I	5′-CAC CTC CGC GGA CAG **GCG GCC GC**C AGG GCT CAT CAC CC-3′	nt 1150−1187 of PUCA-I_N* vector, intron 3 of apoA-I gene
AI*Xho*I	5′-TCC TCT AGA **GTC GAC** CGG CCT TG**C TCG AG**C CCC TTT-3′	nt 2168−2203 of PUCA-I^*_N vector, at 3′-end of apoA-I gene
23S	5′-GTG GAC GCG CTG CGC ACG CAT CTG GCC ... ... GCG CGC CTT GAG GCT CTC AAG GAG AAC-3′	nt 538−564 + nt 598−624 (sense) (amino acids +156 to +164 and amino acids +176 to +184)
23A	5′-GTT CTC CTT GAG AGC CTC AAG GCG CGC ... ... GGC CAG ATG CGT GCG CAG CGC GTC CAC-3′	nt 624−598 + nt 564−538 (antisense) (amino acids +184 to +176 and amino acids +164 to +156)

[a] The restriction enzyme recognition sites are marked in boldface type. [b] nt, nucleotide number of the published apoA-I cDNA sequence (*57*), oligonucleotide position (+) relative to the translation initiation ATG codon. [c] Amino acid position (+) refers to the mature plasma apoA-I sequence. [d] Deleted nucleotides are underlined.

findings are consistent with a model of lipid efflux that requires direct association between the central amphipathic helices of apoA-I and ABCA1.

EXPERIMENTAL PROCEDURES

Materials. DNA modifying enzymes were purchased from New England Biolabs, Inc. (Beverly, MA). Oligonucleotides for polymerase chain reaction (PCR), DH10Bac competent cells, cell culture reagents, rTEV protease, and LipofectAMIN-2000 were purchased from Invitrogen Corp. (Carlsbad, CA). 1,2[^{3}H]Cholesterol (1 mCi/mL; specific activity range, 40−60 Ci/mmol), methyl[^{3}H]choline chloride (1 mCi/mL; specific activity range, 60−90 Ci/mmol), Na^{125}I (5 mCi; specific activity, ∼17 Ci/mg), and materials for PCR were obtained from Perkin-Elmer Life Sciences, Inc. (Boston, MA). Ni-nitrilotriacetic acid resin was purchased from Qiagen, Inc. (Valencia, CA). HiTrap Q HP columns, HiPrep Sephacryl S-200 column, and GammaBind Plus Sepharose (GammaBind G Sepharose) resin were from Amersham Biosciences (Piscataway, NJ). cpt-cAMP and BSA were from Sigma Aldrich Corp. (St. Louis, MO). Cross-linkers DSP and DFDNB, IODO Beads iodination reagent, and D-Salt Dextran plastic desalting columns were obtained from Pierce (Rockford, IL). All other reagents were purchased from Sigma Aldrich Corp., Bio-Rad (Hercules, CA), Fisher Scientific International, Inc. (Suwanee, GA), or other standard commercial sources.

Generation and Isolation of Recombinant WT ApoA-I or ApoA-I Mutants Using the Baculovirus Expression System. To generate baculoviruses expressing WT and mutant apoA-I forms, a *Bam*HI-*Sal*I fragment containing human apoA-I cDNA was cloned into the polylinker region of pFASTBAC donor plasmid that contains the ampicillin and gentamycin resistance genes (Invitrogen Corp.). This recombinant plasmid also contains a histidine (His) tag and the TEV protease cleavage site. The apoA-I containing plasmid was used to transform DH10Bac *Escherichia coli* cells. These cells had been transformed previously with the baculovirus genome containing the *lac*Z and kanamycin resistance genes, along with a helper plasmid containing the tetracycline resistance gene and the transposase genes. Transposition of the apoA-I gene into the *lac*Z gene disrupts the expression of the LacZ and provides a recombinant plasmid named bacmid.

The generation of the donor plasmid expressing WT apoA-I and of plasmids expressing apoA-I[Δ(1−41)], apoA-I[Δ(1−59)], apoA-I[Δ(185−243)], apoA-I[Δ(1−41)Δ(185−243)], apoA-I[Δ(1−59)Δ(185−243)], apoA-I[Δ(136−143)], apoA-I[Δ(144−165)], apoA-I[D102A/D103A], apoA-I[E125K/E128K/K133E/E139K], apoA-I[L141R], and apoA-I[R160V/H162A] mutants was described previously (*21*−*24*). The apoA-I[Δ(89−99)] mutant form of apoA-I was produced in a similar manner. Briefly, the human apoA-I cDNA was mutagenized by PCR, using a set of flanking universal primers 5′-(AIWC-5) and 3′-(AIWC-3) containing the restriction sites *Bam*HI and *Sal*I, a set of mutagenic primers 5′-(AIMIII1−5) and 3′-(AIMIII1−3), and the pBluescript-AI cDNA plasmid as a template. The primers used are shown in Table 1. The DNA fragment containing the mutation of interest was digested with *Bam*HI and *Sal*I and cloned into the corresponding sites of pFASTBAC donor plasmid. For the generation of apoA-I[Δ(61−78)], the 5′-(AIMII1−5) primer that contains the restriction site *Bam*HI and the 3′-(AIMII1−3) primer that contains the 61−78 deletion and the restriction site *Bsu*36I (Table 1) were used in PCR amplification using the pBluescript-AI cDNA plasmid as a template. The amplified segment was digested with *Bam*HI and *Bsu*36I to generate a 208 bp fragment. A 560 bp fragment was also obtained by digestion of pBluescript-AI cDNA plasmid with *Bsu*36I and *Sal*I. The 208 bp and 560 bp fragments and the pFASTBAC donor plasmid, digested with *Bam*HI and *Sal*I, were joined in a triple ligation reaction. Cells containing recombinant bacmids were selected by kanamycin, tetracycline, and gentamycin resistance as white

colonies due to the disruption of *lac*Z sequence in the recombinant bacmid. Recombinant bacmid DNA was isolated from minipreps and used to transfect a monolayer of Sf-9 insect cells (*25*−*27*). Recombinant viruses were isolated, amplified, titrated, and used to infect larger Sf-9 cell cultures grown in suspension at 27 °C. Sf-9 cells were pelleted and resuspended in a lysis buffer. The supernatant was used for the purification of apoA-I fusion proteins (His^+-apoA-I) using a Ni-nitrilotriacetic acid affinity column (*28*, *29*). The pure apoA-I without the His tag (His^--apoA-I) was obtained by cleavage with rTEV protease and purified by using again the Ni-nitrilotriacetic acid affinity chromatography.

Expression and Purification of Recombinant WT and Mutant ProapoA-I Isoforms in C127 Cells. Construction of plasmids expressing WT proapoA-I, proapoA-I[Δ(198−243)], and proapoA-I[Δ(209−243)] has been described previously (*21*, *30*, *31*). The proapoA-I[Δ(165−175)] deletion mutant was constructed in a similar manner. Briefly, the fourth exon of the human apoA-I gene was amplified and mutagenized by the PCR, using a set of specific mutagenic primers (23S, 23A) containing the mutation of interest and a set of flanking universal primers (AI*Not*I, AI*Xho*I) containing the restriction sites *Not*I and *Xho*I, respectively. The sequences of the primers are shown in Table 1. The pUCA-I_N* vector, which contains a *Not*I site in intron 3 and a *Xho*I site in the 3′-end of the apoA-I gene, was used as a template in the amplification reactions (*32*). The DNA fragment containing the mutation of interest was digested with *Not*I and *Sal*I and cloned into the *Not*I and *Xho*I sites of the pBMT3X-AI vector.

Permanent cell lines in mouse mammary tumor C127 cells expressing the WT proapoA-I, the carboxy-terminal truncations proapoA-I[Δ(198−243)] and proapoA-I[Δ(209−243)], and the internal deletion apoA-I[Δ(165−175)] were generated as described previously (*32*). C127 cell clones overproducing the WT and the variant apoA-I forms were grown in roller bottles on collagen-coated lead microspheres (Verax Corp.), and the proteins were purified from the serum-free medium using 5 mL HiTrap Q HP ion exchange columns and Hi-Prep Sephacryl S-200 gel filtration columns as described previously (*32*).

Expression of WT and Mutant ProapoA-I Isoforms in an Adenovirus System. The generation of recombinant adenoviruses carrying the genomic sequence for the WT proapoA-I, proapoA-I[Δ(220−243)], and proapoA-I[Δ(232−243)] has been described before (*21*, *31*).

For apoA-I production, human HTB13 cells (SW 1783, human astrocytoma grown to 80% confluence in Leibovitz's L-15 medium containing 10% (v/v) FBS in roller bottles) were infected with adenoviruses expressing WT proapoA-I, proapoA-I[Δ(220−243)], and proapoA-I[Δ(232−243)] at a multiplicity of infection of 20. After 24 h of infection, cells were washed twice with serum-free medium and preincubated in serum-free medium for 30 min, and fresh serum-free medium was added. After 24 h, the medium was harvested and fresh serum-free medium was added to the cells. The harvests were repeated 8−10 times. The proteins were purified from the serum-free medium by ion exchange chromatography followed by gel filtration, as described above for the C127 cells.

Iodination of ApoA-I. ApoA-I was labeled by ^{125}I using the Iodo-Beads iodination reagent (*33*) and $Na^{125}I$. For each reaction, we used 0.5 mCi of $Na^{125}I$, 0.5 mg of apoA-I ,and two beads as described (*34*). The specific activity was calculated based on the protein concentration, measured by the Bradford protein assay, and the ^{125}I counts and expressed as cpm/ng protein. Specific activities of 200−500 cpm/ng protein were obtained.

Cross-Linking Assay. HEK293-EBNA-T cells were grown in DMEM (high glucose) with 10% (v/v) FBS and antibiotics (*20*, *35*). On day 0, the cells were plated on 12 well plates coated with poly-D-lysine at a density of 2×10^5 cells/well in the same medium without antibiotics. On day 3, cells at about 95% confluence were transfected with LipofectAMIN 2000 and ABCA1 or pcDNA1 (mock) (Invitrogen Corp.) plasmids for 24 h, as recommended by the manufacturer. The DNA-LipofectAMIN 2000 complexes were formed in serum-free opti-MEM I. On day 4, the cells were incubated in DMEM (high glucose)/0.2% (w/v) fatty acid free BSA/antibiotics with ^{125}I-labeled WT or mutant forms of apoA-I at the indicated concentrations at 37 °C for 1 h in the presence or absence of 30-fold molar excess of unlabeled apolipoproteins. The cells were then placed on ice for 15 min and washed three times with PBS. DSP or DFDNB was dissolved immediately before use in dimethyl sulfoxide and diluted to 250 μM with PBS, and 2 mL was added per well. The DSP cross-linker contains thiol sensitive bonds, whereas the DFDNB does not. Cells were incubated at room temperature for 1 h; the medium was removed, and the cells were washed twice with PBS. Cells were lysed at 4 °C with radioimmunoprecipitation buffer (50 mM Tris, pH 7.6, 150 mM NaCl, 0.25% sodium deoxycholate, 1% Nonidet P-40) containing a mixture of protease inhibitors (Roche Molecular Biochemicals, GmbH, Germany) and 1 mM phenylmethylsulfonyl fluoride. Aliquots of 5 μL were kept for determination of cellular protein concentration using the Bradford protein assay. For immunoprecipitation, the cell lysates were centrifuged at 1000*g* in a microcentrifuge for 10 min. The supernatant was collected, 10 μL of GammaBind G Sepharose was added to it, and the mixture was rotated at room temperature for 1 h. After a brief spin, 50 μg of polyclonal anti-ABCA1 antibody was added to the preabsorbed cell lysates and incubated by rotating at room temperature for 2 h. Twenty microliters of GammaBind G Sepharose was then added, and the incubation was continued for 1 h by rotating the tubes. The samples were centrifuged briefly, and the pellet was washed three times with radioimmunoprecipitation buffer. The bound proteins were eluted from the agarose beads by incubation and boiling with Laemmli sample buffer in the presence of 5% β-mercaptoethanol. The eluted proteins were loaded onto 12% gradient SDS-polyacrylamide gel for electrophoresis. Finally, the gel was dried and analyzed for radioactivity in a PhosphorImaging STORM860 system (Molecular Dynamics, Inc., Sunnyvale, CA). The quantitation of the intensities of the bands was performed using the ImageQuant software.

Phosphor pixels of the cross-linked apolipoproteins were converted to fmol of apolipoprotein using equations derived from a standard curve of known amounts of the labeled apolipoproteins imaged in parallel. To calculate the apparent K_d for complex formation of ABCA1 with WT or mutant forms of apoA-I, the fmol of cross-linked apolipoprotein per mg of total cellular protein were plotted vs the initial concentrations of the apolipoprotein. The data were fitted

by nonlinear regression to a one site binding model, using the Prism software (GraphPad Software, Inc.). To obtain the specific cross-linking curves, the residual cross-linking of apoA-I in the presence of 30-fold molar excess of unlabeled apolipoprotein was subtracted from the total cross-linking in the absence of unlabeled apolipoprotein.

Competition assays were carried out as described above for direct cross-linking experiments, except that 1 μg/mL (0.036 μM) of ^{125}I-labeled plasma apoA-I was added to the cells together with unlabeled WT apoA-I or mutant forms at various concentrations. The 100% value corresponds to cross-linking of 1 μg/mL of ^{125}I-labeled plasma apoA-I in the absence of competitor. The value that corresponds to the cross-linking of ^{125}I-plasma apoA-I in the presence of competitor was calculated as a percent of the value in the absence of competitor. When competition was determined at different concentrations of WT apoA-I or mutant forms, the cross-linking of ^{125}I-labeled plasma apoA-I to ABCA1 in the presence of competitors vs the logarithm of the concentration of the competitor was plotted, and the data were fitted by nonlinear regression to a one site competition model, using the Prism software.

Lipid Efflux Assays. J774 mouse macrophages were grown in RPMI 1640 with 10% (v/v) FBS and antibiotics. J774 macrophages were plated in 12 well plates at a density of 5 $\times$ 10^5 cells/well. The following day, cells were labeled with 1 mL of labeling medium (6 μCi/mL 1,2[^{3}H]cholesterol or 1 μCi/mL methyl[^{3}H]choline chloride) for 24 h. Following 24 h of labeling and washing, cells were treated with serum-free medium and equilibrated for 24 h with or without 0.3 mM cpt-cAMP. At the end of the treatment period with cpt-cAMP, cells were washed twice and incubated with 1 mL of RPMI 1640, supplemented with 0.2% (w/v) BSA, with or without 1 μM WT apoA-I or mutant forms at 37 °C. For cholesterol efflux experiments, at different time points up to 6 h, 55 μL of medium was collected and clarified by centrifugation in a microcentrifuge for 2 min. The radioactivity in 40 μL of the supernatant was determined by liquid scintillation counting. For phospholipid efflux experiments, after 4 h of incubation, the media were collected and clarified by centrifugation in a microcentrifuge for 2 min. A 100 μL aliquot of the supernatant was first extracted with chloroform and methanol (*36*), and then, the radioactivity of the chloroform phase was determined by liquid scintillation counting. At the end of the incubation, cells were lysed by 800 μL of lysis buffer (PBS containing 1% (v/v) Triton X-100) for 30 min at room temperature. Radioactivity was measured in 40 μL of cell lysate for cholesterol efflux experiments and in 100 μL of lysate, following extraction (*36*), for phospholipid efflux experiments. The percentage of secreted [^{3}H]lipid was calculated by dividing the medium-derived counts by the sum of the total counts present in the culture medium and the cell lysate. To calculate the net cpt-cAMP-dependent efflux, the lipid efflux of the untreated cells was subtracted from the lipid efflux of the cells treated with cpt-cAMP.

RESULTS

Production of WT and Mutant ApoA-I Forms Used in the Current Studies. The WT and the variant apoA-I forms were produced using three different expression systems (baculovirus, adenovirus, and permanent cell lines). Table 2 describes the apoA-I forms used in this study, the expression system used for their production, and their physicochemical properties. The location of the deletions and point mutations in the apoA-I helices as defined by computer modeling, X-ray crystallography, and physicochemical studies is shown in Figure 1 (*22*, *37*, *38*).

Effect of Amino-Terminal, Carboxy-Terminal, and Double Amino- and Carboxy-Terminal Deletions of ApoA-I on the Ability of ApoA-I to Cross-Link to ABCA1. To explore the functional interactions between apoA-I and ABCA1, we tested the ability of amino-terminal, carboxy-terminal, and double amino- and carboxy-terminal deletion mutants of apoA-I to cross-link to ABCA1.

To test the effect of the above apoA-I mutants on the formation of a molecular complex between apoA-I and ABCA1, we performed competitive cross-linking assays as described in the Experimental Procedures. For immunoprecipitation of the apoA-I/ABCA1 complex, we used a rabbit polyclonal anti-ABCA1 antibody. To exclude nonspecific precipitation, we also used preimmune rabbit IgGs (Figure 2A). It was shown that the amino-terminal deletion mutants apoA-I[Δ(1−41)] and apoA-I[Δ(1−59)] competed effectively the cross-linking of plasma apoA-I to ABCA1. The carboxy-terminal deletion mutants apoA-I[Δ(185−243)], apoA-I[Δ(198−243)], and apoA-I[Δ(209−243)] competed moderately (64−72% as compared to 85−95% for the WT apoA-I produced by the various expression systems). The carboxy-terminal deletion mutant apoA-I[Δ(220−243)] competed poorly (16%). These differences in competition for the cross-linking of plasma apoA-I may be related to alteration in the secondary structure of these mutants as a result of the carboxy-terminal deletions (Table 2). Efficient competitors were also the carboxy-terminal deletion mutant apoA-I[Δ(232−243)] and the double amino- and carboxy-terminal deletion mutants apoA-I[Δ(1−41)Δ(185−243)] or apoA-I[Δ(1−59)Δ(185−243)] (Figure 2A). We have shown recently that the ABCA1-mediated lipid efflux was diminished by carboxy-terminal deletions, was reduced slightly by amino-terminal deletions, and was nearly restored to the WT apoA-I value in mutants lacking both the amino- and the carboxy-terminal regions (*21*).

The ability of selected apoA-I mutants to compete for the cross-linking of plasma apoA-I to ABCA1 was also monitored as a function of their concentration as described in the Experimental Procedures. This analysis showed that the WT apoA-I produced by the baculovirus or the adenovirus system had similar EC_{50} values (140 and 151 nM, respectively). The carboxy-terminal deletion mutant apoA-I[Δ(185−243)] and especially the apoA-I[Δ(220−243)] mutant form had much higher EC_{50} values (389 and 1917 nM, respectively), while the double deletion mutant of both amino- and carboxy-terminal regions of apoA-I had smaller EC_{50} values (EC_{50} of 52 nM for the double deletion mutant similar to the EC_{50} of 58 nM for the plasma apoA-I) (Figure 2B).

To confirm the formation of a complex between the various apoA-I mutants and ABCA1, we iodinated amino-, carboxy-, and double amino- and carboxy-terminal deletion mutants of apoA-I and tested their ability to cross-link to ABCA1 as described in the Experimental Procedures. Figure 2C shows the direct cross-linking of iodinated WT and mutant forms of apoA-I (0.2 μM) to ABCA1 in the presence

Table 2: List of the Variant ApoA-I Forms Used in ABCA1-Mediated Lipid Efflux and Cross-Linking Studies, Expression Systems Used for Their Production, Their Secondary Structure, and Physicochemical Properties (*21*, *22*, *30*)

apoA-I form	expression system	α-helix (%)	estimated no. of α-helical residues altered[a]	free energy of stabilization $\Delta G_D°$ (kcal/mol)	effective enthalpy of thermal denaturation ΔH_v (kcal/mol)	tryptophan environment
WTa apoA-I	baculovirus					
WTb apoA-I	permanent cell lines					
WTc apoA-I	adenovirus					
apoA-I[Δ(1−41)]	baculovirus	0	∼−20	−1.1	−12	
apoA-I[Δ(1−59)]	baculovirus					
apoA-I[Δ(61−78)]	baculovirus					
apoA-I[Δ(89−99)]	baculovirus					
apoA-I[D102A/D103A]	baculovirus					
apoA-I[E125K/E128K/ K133E/E139K]	baculovirus	+7	+17	+0.6	0	
apoA-I[L141R]	baculovirus	0	−5	−0.3	−3	
apoA-I[Δ(136−143)]	baculovirus	+3	∼+2	+0.7	0	
apoA-I[R160V/H162A]	baculovirus					
apoA-I[Δ(144−165)]	baculovirus	−4	0	−0.5	−14	Trp residues are in more polar environment than WT apoA-I
apoA-I[Δ(165−175)]	permanent cell lines	−20	∼−45	−0.9	−26	Trp residues are masked or in more negatively charged environment than WT apoA-I
apoA-I[Δ(185−243)]	baculovirus	0	∼+16	0	0	
apoA-I[Δ(198−243)]	permanent cell lines	−11	∼−12	−0.5	−13	
apoA-I[Δ(209−243)]	permanent cell lines	0	∼+4	−0.5	0	
apoA-I[Δ(220−243)]	adenovirus					
apoA-I[Δ(232−243)]	adenovirus					
apoA-I[Δ(1−41)Δ(185−243)]	baculovirus	−7	∼−25	−1.1	−11	
apoA-I[Δ(1−59)Δ(185−243)]	baculovirus					

[a] On the basis of 58% α-helical content of WT apoA-I, the number of residues in α-helical structure of the WT apoA-I was calculated to 144. The estimation of the number of residues in α-helix for the mutants was as follows: The % α-helical content of each mutant was converted to number of α-helical residues. This number was increased by the number of deleted α-helical residues estimated based on the secondary structure model of apoA-I in Figure 1. The difference (+ or −) of this number from 144 represents the estimated number of α-helical residues altered.

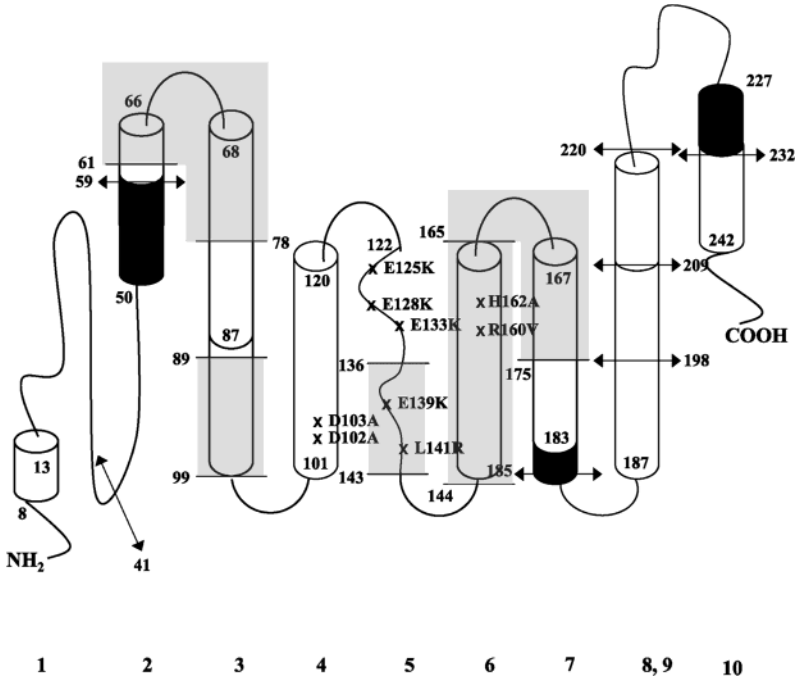

FIGURE 1: Schematic representation of the boundaries of the α-helical regions of apoA-I based on computer modeling (*37*), X-ray crystallography (*38*), and physicochemical studies (*22*). Cylinders represent amphipathic α-helices. Predicted amphipathic α-helices are shown in white; additional α-helical regions that were observed by X-ray crystallography are shown in black. The figure shows the various apoA-I mutants used in this study. Horizontal double arrows ↔ show the sites of amino- and carboxy-terminal deletions, gray areas show the internal deletions, and × indicates point mutations.

or absence of 30-fold molar excess of unlabeled apoA-I. As shown at 30-fold molar excess, the WT apoA-I, the amino-terminal, and the double amino- and carboxy-terminal deletion mutants compete completely the binding of labeled apoA-I, whereas the two carboxy-terminal deletion mutants compete partially. Figure 2D,E shows the cross-linking of WT apoA-I and carboxy-terminal deletion mutants to ABCA1 at different concentrations of labeled apoA-I, which

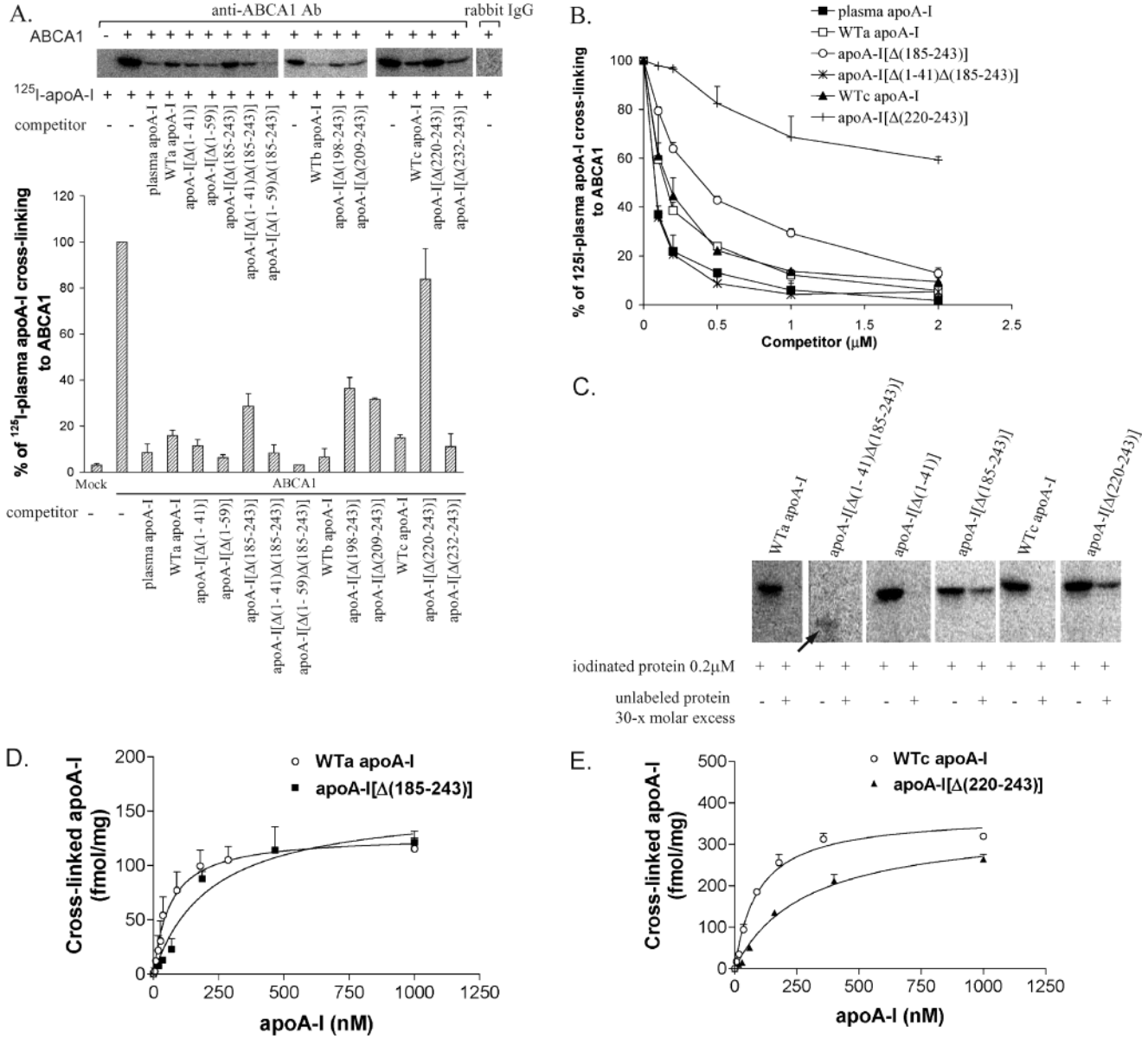

FIGURE 2: Cross-linking of WT apoA-I and amino-terminal, carboxy-terminal, and double amino- and carboxy-terminal deletion mutants of apoA-I to ABCA1. (A) Competition of cross-linking of ^{125}I-apoA-I to ABCA1 by WT and mutant forms of apoA-I at 30-fold molar excess. HEK293 cells transfected with empty vector (mock) or with WT ABCA1 plasmid were incubated for 1 h at 37 °C with 0.036 μM ^{125}I-plasma apoA-I alone or in the presence of a 30-fold molar excess of the indicated unlabeled apolipoproteins. The cells were exposed to the DSP cross-linker, and the apoA-I/ABCA1 complex was immunoprecipitated with a rabbit anti-ABCA1 polyclonal antibody or preimmune rabbit IgG as described in the Experimental Procedures section. The associated apoA-I was visualized and quantitated by phosphor imaging. The value for cross-linking of 0.036 μM ^{125}I-plasma apoA-I in the absence of competitor was set to 100%. The value for cross-linking of ^{125}I-plasma apoA-I in the presence of competitor was calculated relative to the value in the absence of competitor. The immunoprecipitated apoA-I is shown in the top of panel A, and the percent apoA-I/ABCA1 complex formation in the presence or absence of competitor is graphed below. Values are the means ± SD from three independent experiments performed in duplicate. (B) Competition of cross-linking of ^{125}I-apoA-I to ABCA1 by WT and mutant forms of apoA-I at various concentrations. Cross-linking in ABCA1 transfected HEK293 cells was carried out as described in panel A. The value that corresponds to the cross-linking of ^{125}I-plasma apoA-I in the presence of competitor was calculated relative to the value in the absence of competitor, which was set to 100%. Values are the means ± SD from two independent experiments performed in duplicate. Where no error bar is shown, the SD falls within the size of the symbol. (C) Cross-linking of ^{125}I-labeled WT and mutant forms of apoA-I to ABCA1. HEK293 cells transfected with WT ABCA1 plasmid were incubated for 1 h at 37 °C with 0.2 μM ^{125}I-labeled WT or the indicated mutant forms of apoA-I alone or in the presence of a 30-fold molar excess of the respective unlabeled apolipoproteins. Cross-linking with the DSP cross-linker and immunoprecipitation of ABCA1 were carried out as described in panel A. The associated apoA-I was visualized by phosphor imaging. (D, E) Concentration-dependent cross-linking of ^{125}I-labeled WT and mutant forms of apoA-I to ABCA1. Cross-linking in ABCA1 transfected HEK293 cells was carried out as described in panel A. Panels D and E show the specific cross-linking curves for WT apoA-I and the carboxy-terminal deletion mutants. Phosphor pixels of the cross-linked apolipoproteins were converted to fmol of apolipoprotein using equations derived from curves of known amounts of the labeled apolipoproteins imaged in parallel. The cross-linking values of the saturation curves were expressed as fmol of apoA-I associated with ABCA1 per mg of total cellular protein. Values shown are representative of two independent experiments performed in duplicate. Error bars represent the range of duplicate determinations. Where no error bar is shown, the error bar falls within the size of the symbol. In panels C−E, the specific activity of the ^{125}I-labeled apolipoproteins was in the range of 200−500 cpm/ng protein. The ^{125}I labeling of the double deletion mutant apoA-I[Δ(1−41)Δ(185−243)], which contains three Tyr residues is reduced as compared to WT apoA-I, which contains seven Tyr residues. The position of the labeled double deletion mutant is indicated by an arrow.

allowed estimation of the affinity of binding. This analysis showed that the WT apoA-I produced by the baculovirus and adenovirus expression system had apparent K_d values of 64 ± 9 and 94 ± 16 nM, respectively (Figure 2D,E). Similar K_d values for recombinant WT apoA-I have been reported previously (*11*). The apparent K_d values for the amino-terminal deletion mutant apoA-I[Δ(1−41)] and the double amino- and carboxy-terminal deletion mutant apoA-I[Δ(1−41)Δ(185−243)], produced by the baculovirus system, were 49 ± 12 and 74 ± 18 nM, respectively (data not shown). Consistent with the competition data, the apparent K_d values of the carboxy-terminal deletion mutants apoA-I[Δ(185−243)] and apoA-I[Δ(220−243)], produced by the baculovirus and the adenovirus system, were 219 ± 20 and 286 ± 54 nM, respectively (Figure 2D,E).

Effect of Deletions and Point Mutations in Central Helices of ApoA-I on ABCA1-Mediated Lipid Efflux and on the Ability of ApoA-I to Cross-Link to ABCA1. The fact that the carboxy-terminal deletion mutants of apoA-I are defective in ABCA1-mediated lipid efflux and cross-linking, but deletion of both the amino- and carboxy-terminal regions of apoA-I restores the ABCA1-mediated lipid efflux and the cross-linking to the receptor, led us to investigate whether there is a specific amino acid sequence in the central region of the apoA-I that is involved in the apoA-I/ABCA1 interactions. To achieve this, we tested various deletions and point mutations in the central helices of apoA-I for their effect on lipid efflux and their ability to compete the cross-linking of ^{125}I-labeled plasma apoA-I to ABCA1 as described in the Experimental Procedures.

We have shown previously that the ABCA1-mediated lipid efflux to WT and mutant apoA-I forms provides identical results using either cultures of J774 mouse macrophages stimulated by cAMP analogues or cultures of HEK293 cells following transfection with an ABCA1 expressing plasmid (*21*). The net cpt-cAMP-dependent cholesterol or phospholipid efflux in J774 mouse macrophages was obtained by subtracting the efflux values of the untreated cells from the treated cells. The efflux values obtained for WT apoA-I at 4 h were set to 100%. As compared to WT-apoA-I, the cpt-cAMP-dependent cholesterol efflux was not affected in the presence of apoA-I[Δ(61−78)] (deletion of part of helix 2 and helix 3 and the loop connecting them) and apoA-I[Δ(136−143)] (deletion of second half of the 122−144 repeat) and was moderately decreased, 20−30%, in the presence of apoA-I[Δ(89−99)] (deletion of last one-third segment of helix 3), apoA-I[Δ(144−165)] (deletion of the entire helix 6), and apoA-I[Δ(165−175)] (deletion of first half of helix 7) (Figures 1 and 3A, shaded bars). The cpt-cAMP-dependent phospholipid efflux was not affected in the presence of apoA-I[Δ(61−78)], apoA-I[Δ(136−143)], and apoA-I[Δ(165−175)] and decreased by 44% in the presence of apoA-I[Δ(89−99)] and by 24% in the presence of apoA-I[Δ(144−165)] mutant (Figure 3B, shaded bars). When the internal deletion mutants of apoA-I were tested for their ability to compete for the cross-linking of plasma apoA-I to ABCA1 in cells expressing ABCA1, all mutants competed strongly (Figure 3C).

The point mutants in apoA-I tested for their effect on apoA-I/ABCA1 interactions were apoA-I[D102A/D103A], apoA-I[R160V/H162A], apoA-I[E125K/E128K/K133E/E139K], and apoA-I[L141R]. The first two mutants were shown previously to have diminished ability to promote SR-BI-mediated lipid efflux (*24*). The third mutant was shown to have increased α-helical content and stability (*22*), and the fourth is a natural apoA-I mutation occurring in humans (*39*, *40*).

These studies showed that as compared to the WT apoA-I, the cpt-cAMP-dependent cholesterol and phospholipid efflux was unaffected by all of the point mutations in apoA-I (Figure 4A,B, shaded bars). All of the point mutants in apoA-I were found to strongly compete the cross-linking of ^{125}I-plasma apoA-I to ABCA1 in cells expressing ABCA1 (Figure 4C).

Overall, these findings show that none of the amino acids sequences in the central region of apoA-I that were tested has a strong effect on ABCA1-mediated lipid efflux or cross-linking to ABCA1. Furthermore, overall, there is a good correlation of ABCA1 cross-linking to lipid efflux for all of the internal deletions and point mutations of apoA-I used in this study.

Effect of Amino-Terminal, Carboxy-Terminal, and Double Amino- and Carboxy-Terminal Deletions of ApoA-I on the Ability of ApoA-I to Cross-Link to the ABCA1[W590S] Mutant. To further explore the interaction of apoA-I with ABCA1, we tested the ability of various apoA-I mutants to associate with the ABCA1[W590S] mutant. In a previous study, it was found that this ABCA1 mutant cross-linked to apoA-I with an efficiency greater than that of WT ABCA1 but was defective in apoA-I-dependent cholesterol efflux (*20*). For this purpose, we performed a direct cross-linking of iodinated WT and mutant forms of apoA-I (0.2 μM) to WT ABCA1 or the ABCA1[W590S] mutant in the presence or absence of 30-fold molar excess of the corresponding unlabeled apoA-I form as described in the Experimental Procedures. As shown in Figure 5A, the WT apoA-I, the amino-terminal, and the double amino- and carboxy-terminal deletion mutants of apoA-I cross-link to ABCA1[W590S] and the cross-linking is completely inhibited by 30-fold molar excess of unlabeled apoA-I. The carboxy-terminal deletion mutants apoA-I[Δ(185−243)] and apoA-I[Δ(220−243)] cross-link less efficiently to either WT ABCA1 or mutant ABCA1[W590S], and the cross-linking is partially competed by 30-fold molar excess of unlabeled apolipoprotein. The WT apoA-I and the apoA-I[Δ(1−41)Δ(185−243)] mutant have higher and equal ability, respectively, to cross-link to ABCA1[W590S] as compared to WT ABCA1. However, the amino-terminal deletion mutant apoA-I[Δ(1−41)] and the carboxy-terminal deletion mutants apoA-I[Δ(185−243)] and apoA-I[Δ(220−243)] show 36−64% reduced cross-linking to ABCA1[W590S] (Figure 5B). The finding suggests subtle differences in the cross-linking of WT and mutant apoA-I forms to the ABCA1[W590S] mutant as compared to the cross-linking of the same apoA-I forms to the WT ABCA1.

Cross-Linking ApoA-I with ABCA1 with a 3 Å Cross-Linker. In a previous study, the 7.7 Å cross-linker DSG was found to be as effective as the 12 Å cross-linker DSP in cross-linking apoA-I to ABCA1 (*20*). In the current study, we tested the ability of the DFDNB cross-linker, which has a spacer arm of 3 Å, to cross-link apoA-I to ABCA1. As it is shown in Figure 6, DFDNB cross-linked apoA-I to ABCA1 as strongly as DSP, indicating that the pair of reactive amino acids of ABCA1 and apoA-I are with a distance of ≤3 Å.

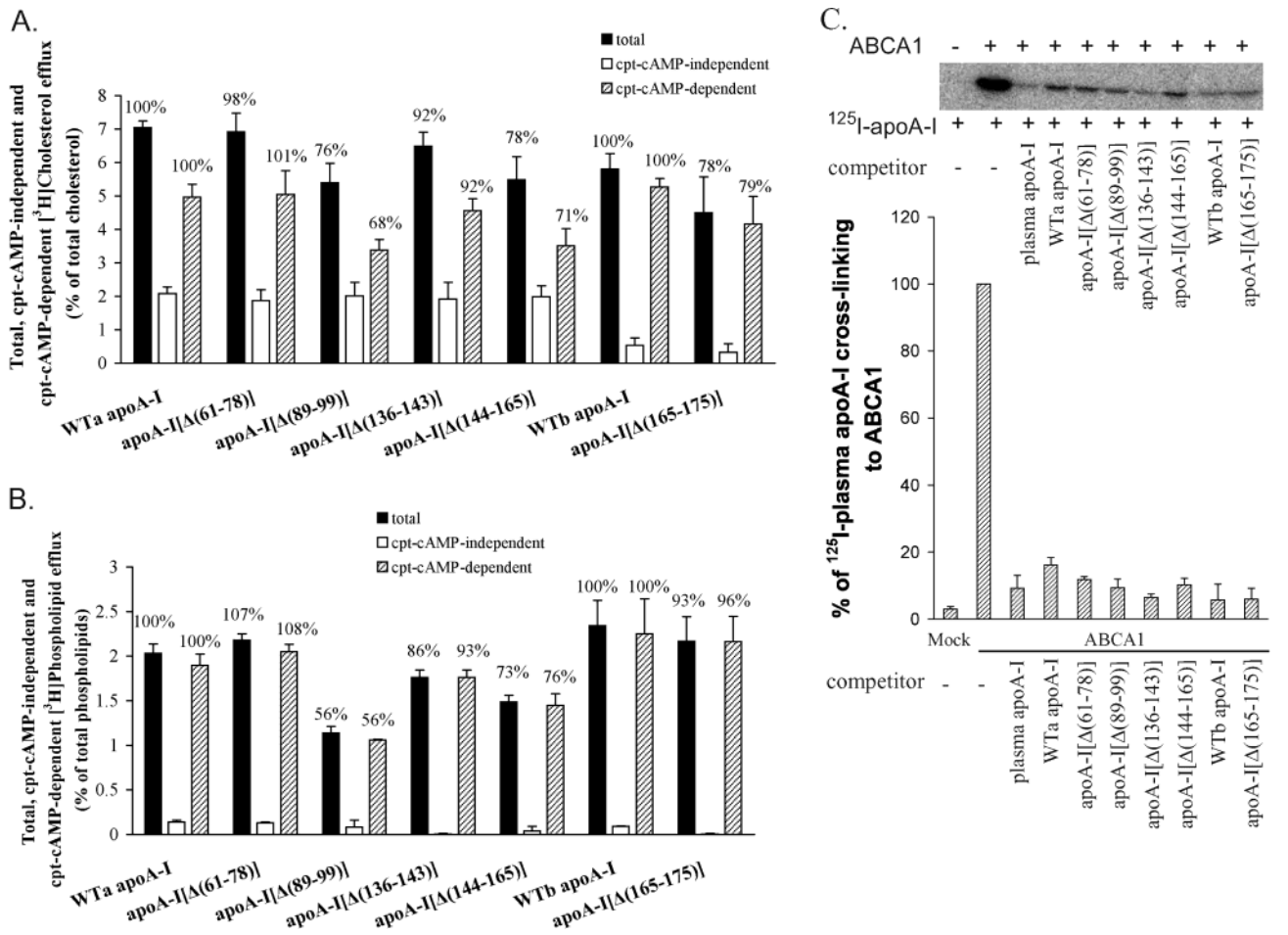

FIGURE 3: ABCA1-mediated lipid efflux and competition of cross-linking of ^{125}I-apoA-I to ABCA1 in the presence of WT apoA-I and internal deletion mutants of apoA-I. (A) Effect of deletions of internal helices of apoA-I on cholesterol efflux from J774 mouse macrophages. Cells labeled with 6 μCi/mL [^{3}H]cholesterol for 24 h and treated for 24 h with or without 0.3 mM cpt-cAMP were incubated with 1 μM WT and mutant forms of apoA-I for 4 h at 37 °C. Media and cells were collected separately, and the radioactivity was measured as described in the Experimental Procedures. The percent of [^{3}H]cholesterol efflux represents the amount of the radioactivity released in the medium divided by the total radioactivity present in the culture medium and the cell lysate. The percent of the net cpt-cAMP-dependent [^{3}H]cholesterol efflux was calculated as the difference in percent of cholesterol efflux between treated cells (total efflux) and untreated cells (cpt-cAMP-independent efflux). Black and white bars show the percent of [^{3}H]cholesterol efflux from cpt-cAMP treated and untreated cells, respectively. Shaded bars show the percent of the net cpt-cAMP-dependent [^{3}H]cholesterol efflux. The numbers on top of the bars represent the cholesterol efflux relative to the WT control set to 100%. Values are the means ± SD from three independent experiments performed in duplicate. (B) Effect of deletion of internal helices of apoA-I on phospholipid efflux from J774 mouse macrophages. Cells labeled with 1 μCi/mL [^{3}H]choline for 24 h and treated for 24 h with or without 0.3 mM cpt-cAMP were incubated with 1 μM WT and mutant apoA-I forms for 4 h at 37 °C. Media and cells were collected separately, the [^{3}H]phospholipids were first extracted, and then, the radioactivity was measured as described in the Experimental Procedures. The results were calculated and graphed as described in panel A. The numbers on top of the bars represent the phospholipid efflux relative to the WT control set to 100%. Values are the means ± SD from two independent experiments performed in duplicate. (C) Competition of cross-linking of ^{125}I-apoA-I to ABCA1 by WT apoA-I and deletion mutants of internal helices of apoA-I at 30-fold molar excess. Cross-linking in ABCA1 transfected HEK293 cells was carried out as described in the legend of Figure 2A. The immunoprecipitated apoA-I is shown in the top of panel C and the percent apoA-I/ABCA1 complex formation in the presence or absence of competitor is graphed below. Values are the means ± SD from two independent experiments performed in duplicate.

DISCUSSION

Background. ApoA-I and ABCA1 are essential for the formation of HDL. Human patients or animal models that lack or have defective forms of apoA-I or ABCA1 fail to form HDL (*5*−*8*, *21*, *31*, *41*−*44*). Although it is clear that functions of both apoA-I and ABCA1 are critical for the biogenesis of HDL, the question that persists is what is the nature of the functional interactions between these two very important proteins?

Two previous models that have been advanced to explain the ABCA1/apoA-I interactions assumed that there is no direct association between ABCA1 and apoA-I. The first model proposed an ABCA1-dependent generation of an unstable membrane domain by flipping phospholipid to the outer leaflet of the plasma membrane. Such phosphatidylserine flipping might allow docking and subsequent lipidation of the amphipathic helices of apoA-I (*11*, *12*). In another version of the first model, it was proposed that following docking, the lipidation of apoA-I involves extraction of membrane phospholipid and cholesterol by microsolubilization (*18*). The second model, designated the hybrid model, is a modification of the first two and proposed that an initial tethering of apoA-I to membranes occurs through the carboxy-terminal apoA-I region and that the membrane-bound apoA-I moves and associates with ABCA1 to accept lipids (*19*).

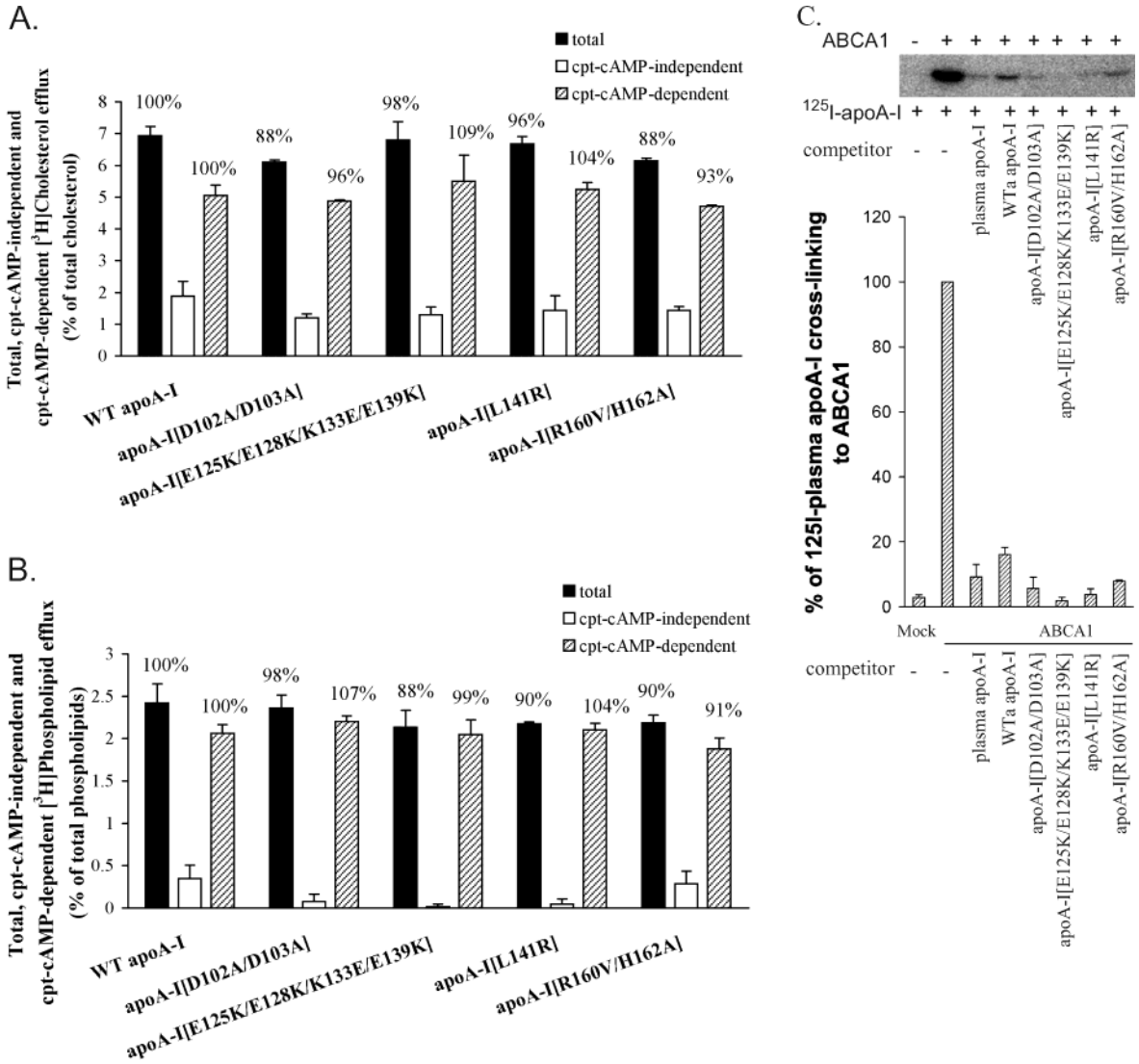

FIGURE 4: ABCA1-mediated lipid efflux and competition of cross-linking of ^{125}I-apoA-I to ABCA1 in the presence of WT apoA-I and point mutants of apoA-I. (A) Effect of point mutations of apoA-I on cholesterol efflux from J774 mouse macrophages. Cholesterol efflux following 4 h of incubation at 37 °C was determined as described in the legend of Figure 3A. Black and white bars show the percent of [^{3}H]cholesterol efflux from cpt-cAMP treated and untreated cells, respectively. Shaded bars show the percent of the net cpt-cAMP-dependent [^{3}H]cholesterol efflux. The numbers on top of the bars represent the cholesterol efflux relative to the WT control set to 100%. Values are the means ± SD from three independent experiments performed in duplicate. (B) Effect of point mutations of apoA-I on phospholipid efflux from J774 mouse macrophages. Phospholipid efflux following 4 h of incubation at 37 °C was determined as described in the legend of Figure 3B. The results were calculated and graphed as described in panel A. The numbers on top of the bars represent the phospholipid efflux relative to the WT control set to 100%. Values are the means ± SD from two independent experiments performed in duplicate. (C) Competition of cross-linking of ^{125}I-apoA-I to ABCA1 by WT apoA-I and point mutants of apoA-I at 30-fold molar excess. Cross-linking in ABCA1 transfected HEK293 was carried out as described in the legend of Figure 2A. The immunoprecipitated apoA-I is shown in the top of panel C and the percent apoA-I/ABCA1 complex formation in the presence or absence of competitor is graphed below. Values are the means ± SD from two independent experiments performed in duplicate.

A third intuitive model is the direct association model, which assumes physical interactions between apoA-I and ABCA1 (*20*, *45*). This model is supported by the observation that, with the exception of a single mutant ABCA1[W590S], all other natural mutants in the two extracellular loops of ABCA1 tested, which are defective in cholesterol efflux, cross-link inefficiently to ABCA1 (*20*). The current study establishes that cross-linking by a reagent with a spacer arm of 3 Å is possible, suggesting that the reactive ABCA1 and apoA-I residues are in very close proximity.

Our recent studies showed that the carboxy-terminal apoA-I mutants that lack the 220−231 region of apoA-I fail to promote ABCA1-dependent lipid efflux indicating that there is a specificity of ABCA1 for the apoA-I acceptor (*21*). To interpret these findings, we suggested that in the full-length apoA-I, physical interactions of the carboxy-terminal domain, which contains residues 220−231, with the amino terminal domain permit functional interactions between full-length apoA-I and ABCA1 and when the residues 220−231 are missing these interactions do not occur. Consistent with this interpretation, recent fluorescence quenching studies support the concept that the amino- and the carboxy-terminal segments of apoA-I are in close proximity (*30*). Furthermore, additional experiments showed that the mechanism of ABCA1/apoA-I interactions was more complex, since deletion of both the amino- and the carboxy-terminal domain

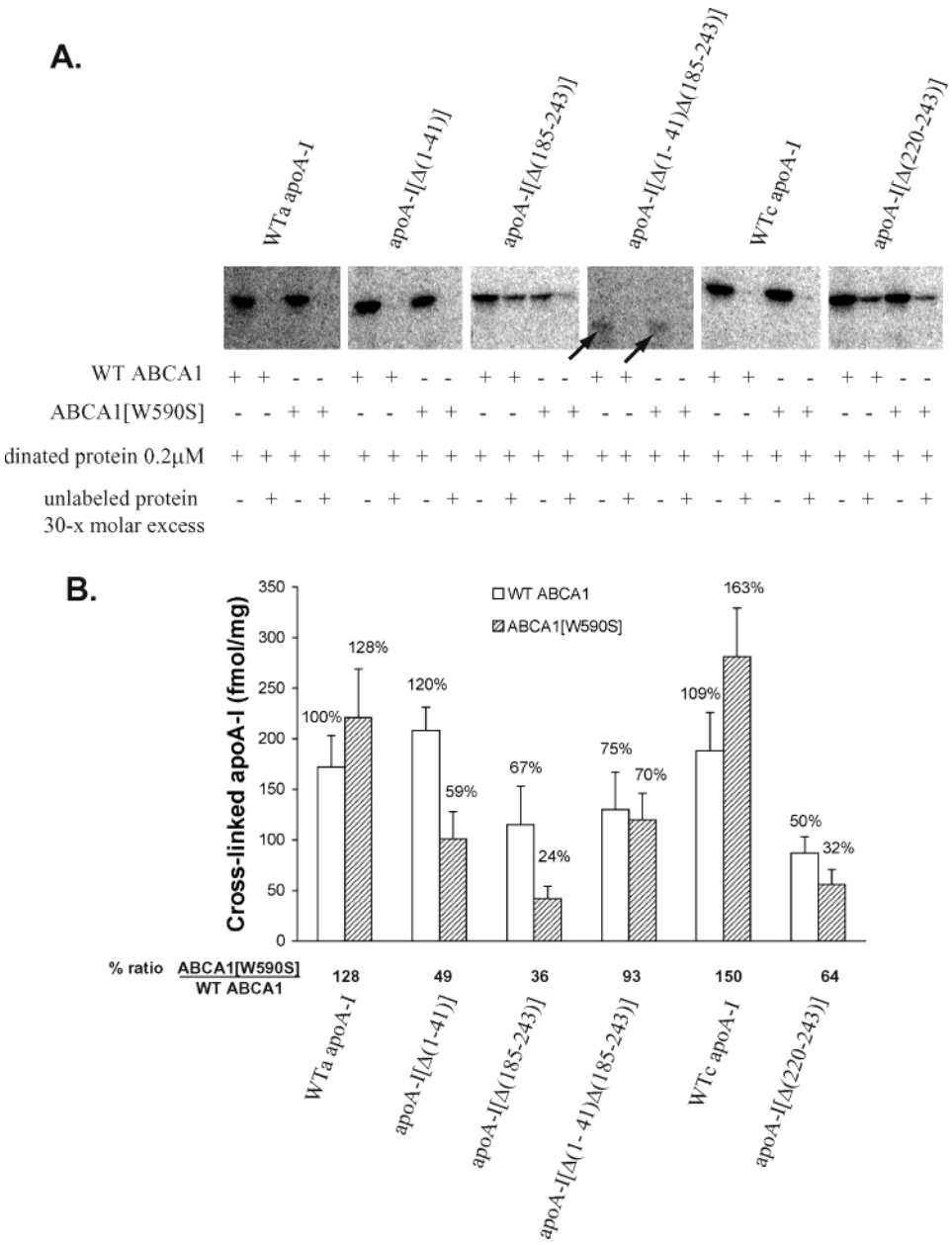

FIGURE 5: Cross-linking of ^{125}I-labeled WT and mutant forms of apoA-I to WT ABCA1 and ABCA1[W590S]. HEK293 cells transfected with plasmids carrying the WT ABCA1 and ABCA1[W590S] mutant were incubated for 1 h at 37 °C with 0.2 μM ^{125}I-labeled WT or the indicated mutant forms of apoA-I alone or in the presence of a 30-fold molar excess of the respective unlabeled apolipoproteins. Cross-linking was carried out as described in the legend of Figure 2A. The resulting immunoprecipitated apoA-I is shown in panel A. The specific activity of the ^{125}I-labeled apolipoproteins was in the range of 200−500 cpm/ng protein. The ^{125}I labeling of the double deletion mutant apoA-I[Δ(1−41)Δ(185−243)], which contains three Tyr residues, is reduced as compared to WT apoA-I, which contains seven Tyr residues. The position of the labeled double deletion mutant is indicated by an arrow. The fmol of cross-linked WT or mutant forms of apoA-I per mg of cellular protein to WT ABCA1 and ABCA1[W590S] were calculated as described in the legend of the Figure 2D,E and are graphed to panel B. Panel B shows the total cross-linking of the indicated apoA-I forms to WT ABCA1 and the ABCA1[W590S] mutant. The value that corresponds to the fmol of cross-linked WTa apoA-I to WT ABCA1 per mg of cellular protein was set to 100%. The cross-linking of WT and mutant forms of apoA-I to the WT and mutant ABCA1 was compared to this 100% value. The % ratio of the cross-linking of each ^{125}I-labeled apoA-I form to the ABCA1[W590S] mutant to the cross-linking of the same apoA-I form to the WT ABCA1 was also calculated and is shown in the lower part of the panel B. Error bars represent the range of duplicate determinations.

that includes residues 220−231 restored cholesterol efflux, thus suggesting that the central helices of apoA-I are sufficient to promote lipid efflux (*21*).

Correlation of Cross-Linking of Amino-, Carboxy-, and Double Deletion Mutants of ApoA-I with Their Cholesterol Efflux Properties and Their Ability to Form HDL: ApoA-I Mutants that Are Poor Cholesterol Acceptors Cross-Link Poorly to ABCA1. Using different expression systems, we have generated a large number of apoA-I mutants that can be assigned in four main categories: (i) amino- or carboxy-terminal deletions; (ii) double deletions of both the amino- and the carboxy-terminal regions; (iii) internal deletions of helices 2, 3, 6, and 7 and the 122−144 repeat; and (iv) point mutations in helices 4 and 6 and the 122−144 repeat. With

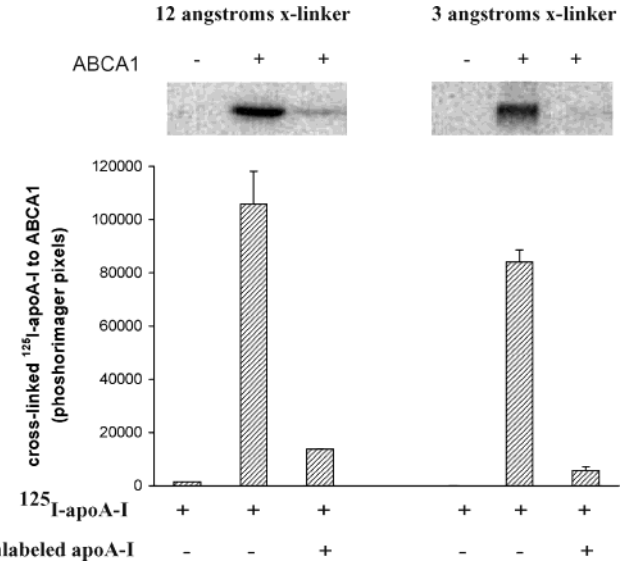

FIGURE 6: Cross-linking of ^{125}I-apoA-I to ABCA1 using the 3 Å cross-linker DFDNB. HEK293 cells transfected with empty vector (mock) or with WT ABCA1 plasmid were incubated for 1 h at 37 °C with 0.036 μM ^{125}I-plasma apoA-I alone or in the presence of a 30-fold molar excess of unlabeled apoA-I. Cross-linking with the indicated cross-linker (DSP and DFDNB) was carried out as described in the legend of Figure 2A. The immunoprecipitated apoA-I is shown in the top panel, and the amount of apoA-I is graphed below. Values are the means ± SD from two independent experiments performed in duplicate.

such extensive mutagenesis, one might expect to identify critical domains or residues of apoA-I, which are required for cholesterol efflux.

Combined competition and direct cross-linking experiments in the current study have shown that the apoA-I[Δ(220−243)] mutant has the lowest binding affinity for ABCA1, followed by the three other carboxy-terminal deletion mutants apoA-I[Δ(185−243)], apoA-I[Δ(198−243)], and apoA-I[Δ(209−243)]. The direct cross-linking and competition properties parallel the cholesterol efflux capacity of the amino-, carboxy-, and double amino- and carboxy-terminal deletion mutants of apoA-I that were studied previously (*21*).

In vivo adenovirus-mediated gene transfer showed that the WT apoA-I and the amino-terminal apoA-I mutant apoA-I[Δ(1−41)] formed spherical HDL particles, the double deletion mutant apoA-I[Δ(1−41)Δ(185−243)] formed discoidal HDL particles, and the carboxy-terminal deletion mutants failed to form HDL (*21*, *31*). These properties of the double deletion mutants of apoA-I also argue against the hybrid model of cholesterol efflux (*19*) that implies binding of apoA-I to the membrane through the carboxy-terminal region prior to its interaction with ABCA1.

Search for Helical Domains and Specific Residues in the Central Region of ApoA-I, Which May Be Essential for ApoA-I/ABCA1 Interactions and Cholesterol Efflux. Given the fact that the central regions of apoA-I are by themselves sufficient to promote cholesterol efflux and HDL biogenesis (*21*), we addressed the question whether specific domains or residues within this region are involved. For this purpose, we used the apoA-I mutants that have either deletions or point mutations within the central region of apoA-I that encompasses helices 2−7. The rationale of using the deletion mutants is obvious. One of the point mutants, apoA-I[E125K/E128K/K133E/E139K], altered four charged amino acids within the 122−144 repeat of apoA-I to amino acids with the opposite charge. Previous physicochemical analysis indicated that this region of apoA-I, which was previously designated as helix 5, lacks defined secondary structure in solution (*22*), whereas the corresponding region of apoE has α-helical structure (*46*). Thus, the amino acid substitutions within the 122−144 repeat were designed to change the residues of apoA-I so that they are identical to the corresponding amino acids of apoE expecting to convert the 122−144 repeat to α-helix. The point mutations apoA-I[D102A/D103A] and apoA-I[R160V/H162A] changed charged amino acids close to the kinks (β-turns) of helices 4 and 6 to neutral amino acids (*37*, *38*). The rationale was that some of these amino acids located at the end of helices may be available to interact with other proteins, such as ABCA1. Finally, the apoA-I [L141R] is a natural apoA-I mutant in humans associated with low HDL levels and premature atherosclerosis (*39*, *40*).

Analysis of the internal deletion and point mutants in the central helices 2−7 of apoA-I showed that all competed efficiently for the cross-linking of WT apoA-I to ABCA1. Their affinity for ABCA1 was paralleled by their capacity to promote efflux of cellular cholesterol and phospholipids. The findings suggest that none of the central helices is an essential domain that determines by itself the ability of apoA-I to associate efficiently to ABCA1 and to promote lipid efflux. Rather, the data indicate that different combinations of central helices can cross-link efficiently to ABCA1 and can promote lipid efflux.

Lack of Correlation of the ABCA1-Dependent Lipid Efflux Capacity of ApoA-I Mutants with Their Secondary Structure in Lipid-Free State. Previous analysis of several apoA-I mutants used in this study provided useful information on the physicochemical properties of the apoA-I variants, which is summarized in Table 2. These mutations either increased, decreased, or did not affect the α-helical content, the stability ($\Delta G_D°$), and the enthalpy of thermal denaturation (ΔH_v) of the different apoA-I mutants and in two cases altered the local environment of Trp residues (Table 2).

Despite these positive and negative changes in the secondary and most likely the tertiary structure of apoA-I, the internal deletion and the point mutants in apoA-I maintained their ability to promote ABCA1-mediated cholesterol efflux. This would suggest that there might not be a strict tertiary structure requirement for the functional interactions of apoA-I mutants with ABCA1. The general feature then that persists is that apoA-I mutants that cross-link efficiently or compete for the cross-linking of WT apoA-I to ABCA1 as well as the WT apoA-I promote cholesterol efflux and those that cross-link or compete less efficiently are poor acceptors in cholesterol efflux and fail to form HDL in vivo (*21*, *31*).

Is There a Specificity of ABCA1 for ApoA-I and Other Ligands? The observation that a variety of apolipoproteins and synthetic peptides of D or L configuration and a large number of apoA-I variants can cross-link with ABCA1 and promote cholesterol efflux (*47*−*49*) suggests that the specificity of ABCA1 for the apoA-I and other cholesterol acceptors is broad. The common feature of these lipid acceptors is that they contain amphipathic α-helices. It is unlikely that a stretch of specific amino acids in the primary sequence of apoA-I or distal residues of apoA-I organized

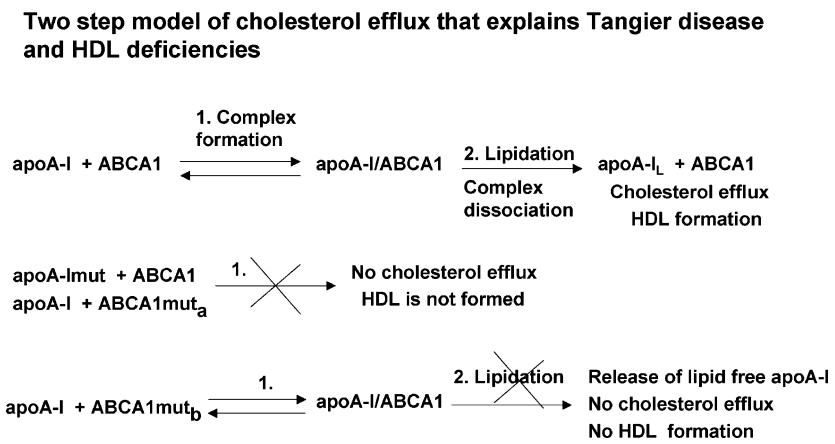

FIGURE 7: Two step model of cholesterol efflux. The first step involves complex formation between apoA-I and ABCA1. The second step involves lipidation of apoA-I and release of the complex. Defects in the two step model of cholesterol efflux that inhibit lipid efflux in vitro and HDL formation in vivo may result either from lack of association due to the mutations in apoA-I or ABCA1 or lack of lipidation of the apoA-I acceptor.

in a precise tertiary structure is required for the functional interactions between apoA-I and ABCA1. Rather, it may be a constant feature of secondary structure of the cholesterol acceptors, such as the amphipathic α-helices of apolipoproteins and peptides, that is required for functional interactions with ABCA1. The combined evidence from this and previous studies (*20*, *21*, *47*−*49*) suggest that such amphipathic α-helices may be responsible for protein−protein interactions between apoA-I and ABCA1 that result in lipid efflux. All of the apoA-I mutants tested in this study maintain 90−150 residues in α-helical structure, which corresponds to a minimum of at least four 22 residue long amphipathic α-helices. Even when these helices exist in a very loose tertiary structure, such as in the apoA-I[Δ(165−175)] deletion mutant (Table 2) (*30*), they can be available to interact with complementary secondary structures present in the active site of ABCA1. The fact that the apoA-I and ABCA1 can form spatially close complexes that can be cross-linked with 3 Å long cross-linker is consistent with this hypothesis. The non-association model would require binding of apoA-I to the cell membrane, 3 Å away from ABCA1 through amphipathic α-helices (*11*, *12*, *18*) and cannot account for the behavior of the carboxy-terminal deletion mutants, which fail to promote cholesterol efflux and to form HDL in vivo despite the fact that they maintain extensive amphipathic α-helical structures (Table 2). The most plausible explanation for the behavior of these mutants is steric hindrance, which may inhibit the formation of an apoA-I/ABCA1 complex.

Interactions of WT and Mutant Forms of ApoA-I with the WT ABCA1 and the ABCA1[W590S] Mutant Differ and May Account for the Inability of the ABCA1[W590S] Mutant, Which Binds Strongly to ApoA-I, To Promote Cholesterol Efflux. The present, as well as a previous study (*20*), showed that the ABCA1[W590S] cross-links better than WT ABCA1 to apoA-I but fails to promote cholesterol efflux in vitro and HDL formation in vivo (*7*, *20*). However, as shown in this study, the amino- and carboxy-terminal deletion mutants cross-link less efficiently to the ABCA1[W590S] mutant, and the double deletion mutant cross-links with similar efficiency to the WT and the mutant ABCA1 forms. These findings suggest that different apoA-I cholesterol acceptors have slight differences in their interactions with the WT and the mutant ABCA1 forms. If the binding of apoA-I acceptors to the ABCA1 [W590S] mutant was brought about by ABCA1-dependent changes in the cell membrane (*11*, *12*), one would expect that apoA-I mutants that bind inefficiently to the WT ABCA1 would also bind inefficiently to the ABCA1[W590S] mutant and vice versa. One possible way then to interpret the inability of the ABCA1[W590S] mutant to promote cholesterol efflux, is to assume that the complex formed is a non-productive complex that prevents the lipidation of apoA-I that is bound to ABCA1. In a non-productive complex, one can envision an apoA-I molecule bound to ABCA1 in an incorrect orientation that prevents the lipidation of apoA-I. In fact, recent experiments have confirmed this hypothesis by showing that following binding to the WT ABCA1, the apoA-I is released associated with cholesterol, whereas apoA-I bound to the ABCA1[W590S] mutant is released in lipid-free form (*49*). Other experiments also showed that lipid efflux can be restored in ABCA1 double mutants by additional mutations that increase the binding of apoA-I (*12*).

A Two Step Model in the ABCA1-Mediated Cholesterol Efflux. Taking together all of the available data, we suggest a two step model of cholesterol efflux that can explain the functional interactions of ABCA1 with apoA-I and other cholesterol acceptors (Figure 7). The first step is a formation of a tight complex between ABCA1 and its ligands. This step is strongly supported by the cross-linking data between WT and mutant forms of ABCA1 and apoA-I as well as with other cholesterol acceptors that contain amphipathic α-helices. Lack of association between ABCA1 and apoA-I variants, formation of a weak complex, or formation of a non-productive complex may prevent lipidation of apoA-I and cholesterol efflux. Formation of a weak complex may, for instance, occur in the case of the carboxy-terminal mutants of apoA-I, which were shown to have reduced affinity for ABCA1 (*21*, *31*), as well as in the case of the various ABCA1 mutants that are associated with Tangier disease (*5*, *6*, *20*, *41*). All of these apoA-I and ABCA1 mutations are associated with defective cholesterol efflux in vitro and the inability to form HDL in vivo (*5*, *6*, *20*, *21*, *31*, *41*).

The second step in cholesterol efflux is the lipidation of HDL and its dissociation from the complex. In the case of the ABCA1[W590S] mutant, the complex is formed but the

apoA-I is not lipidated and is released in a lipid-free form (*49*). The inability of apoA-I bound to ABCA1 to accept lipids may be due to the formation of a non-productive complex that cannot accept phospholipids and cholesterol. Formation of a non-productive complex is supported by our data, which showed that WT and mutant apoA-I have differences in their cross-linking to the WT ABCA1 and the ABCA1[W590S] mutant.

In the case of cholesterol acceptors other than apoA-I, one can also assume similarly a two step model of cholesterol efflux involving complex formation via the amphipathic α-helices and dissociation of the lipidated complex. In the case of the small apolipoproteins apoCII, apoCIII, and apoA-II, following their release from the complex, the lipidated apolipoproteins may attach through their lipid moieties to preexisting lipoproteins. In the case of apoE, the lipidated apoE may proceed to form discoidal and spherical apoE-containing lipoproteins (*50*−*52*). This process may be important for the biogenesis of apoE-containing lipoproteins in the brain where apoE and apoCI are the only apolipoproteins produced in neural cells (*50*, *51*, *53*−*56*).

It is obvious that additional in vivo and in vitro experiments will be necessary to further support the two step model of cholesterol efflux and to decipher the role of ABCA1, apoA-I, and other apolipoproteins in the biogenesis and the functions of lipoproteins in the circulation and the brain.

ACKNOWLEDGMENT

We thank Ms. Gayle Forbes for technical assistance and Ms. Anne Plunkett for typing the manuscript. We also thank Ms. C. A. England and Mr. M. S. Gigliotti for providing the human plasma apoA-I.

REFERENCES

1. Zannis, V. I., Kardassis, D., and Zanni, E. E. (1993) Genetic Mutations Affecting Human Lipoproteins, Their Receptors, and Their Enzymes, *Adv. Hum. Genet. 21*, 145−379.
2. von Eckardstein, A., Nofer, J. R., and Assmann, G. (2001) High-density lipoproteins and arteriosclerosis. Role of cholesterol efflux and reverse cholesterol transport, *Arterioscler. Thromb. Vasc. Biol. 21*, 13−27.
3. Gagescu, R., Demaurex, N., Parton, R. G., Hunziker, W., Huber, L. A., and Gruenberg, J. (2000) The recycling endosome of Madin-Darby canine kidney cells is a mildly acidic compartment rich in raft components, *Mol. Biol. Cell 11*, 2775−2791.
4. Fielding, C. J. (2001) Caveolae and signaling, *Curr. Opin. Lipidol. 12*, 281−287.
5. Lawn, R. M., Wade, D. P., Garvin, M. R., Wang, X., Schwartz, K., Porter, J. G., Seilhamer, J. J., Vaughan, A. M., and Oram, J. F. (1999) The Tangier disease gene product ABC1 controls the cellular apolipoprotein-mediated lipid removal pathway, *J. Clin. Invest. 104*, R25−R31.
6. Brooks-Wilson, A., Marcil, M., Clee, S. M., Zhang, L. H., Roomp, K., van Dam, M., Yu, L., Brewer, C., Collins, J. A., Molhuizen, H. O. F., Loubser, O., Ouelette, B. F. F., Fichter, K., Ashbourne-Excoffon, K. J. D., Sensen, C. W., Scherer, S., Mott, S., Denis, M., Martindale, D., Frohlich, J., Morgan, K., Koop, B., Pimstone, S., Kastelein, J. J. P., Genest, J., Jr., and Hayden, M. R. (1999) Mutations in ABC1 in Tangier disease and familial high-density lipoprotein deficiency, *Nat. Genet. 22*, 336−345.
7. Bodzioch, M., Orso, E., Klucken, J., Langmann, T., Bottcher, A., Diederich, W., Drobnik, W., Barlage, S., Buchler, C., Porsch-Ozcurumez, M., Kaminski, W. E., Hahmann, H. W., Oette, K., Rothe, G., Aslanidis, C., Lackner, K. J., and Schmitz, G. (1999) The gene encoding ATP-binding cassette transporter 1 is mutated in Tangier disease, *Nat. Genet. 22*, 347−351.
8. Rust, S., Rosier, M., Funke, H., Real, J., Amoura, Z., Piette, J. C., Deleuze, J. F., Brewer, H. B., Duverger, N., Denefle, P., and Assmann, G. (1999) Tangier disease is caused by mutations in the gene encoding ATP-binding cassette transporter 1, *Nat. Genet. 22*, 352−355.
9. Oram, J. F., Lawn, R. M., Garvin, M. R., and Wade, D. P. (2000) ABCA1 is the cAMP-inducible apolipoprotein receptor that mediates cholesterol secretion from macrophages, *J. Biol. Chem. 275*, 34508−34511.
10. Wang, N., Silver, D. L., Thiele, C., and Tall, A. R. (2001) ATP-binding cassette transporter A1 (ABCA1) functions as a cholesterol efflux regulatory protein, *J. Biol. Chem. 276*, 23742−23747.
11. Chambenoit, O., Hamon, Y., Marguet, D., Rigneault, H., Rosseneu, M., and Chimini, G. (2001) Specific docking of apolipoprotein A-I at the cell surface requires a functional ABCA1 transporter, *J. Biol. Chem. 276*, 9955−9960.
12. Rigot, V., Hamon, Y., Chambenoit, O., Alibert, M., Duverger, N., and Chimini, G. (2002) Distinct sites on ABCA1 control distinct steps required for cellular release of phospholipids, *J. Lipid Res. 43*, 2077−2086.
13. Fielding, P. E., Nagao, K., Hakamata, H., Chimini, G., and Fielding, C. J. (2000) A two-step mechanism for free cholesterol and phospholipid efflux from human vascular cells to apolipoprotein A-1, *Biochemistry 39*, 14113−14120.
14. Forte, T. M., Goth-Goldstein, R., Nordhausen, R. W., and McCall, M. R. (1993) Apolipoprotein A-I-cell membrane interaction: extracellular assembly of heterogeneous nascent HDL particles, *J. Lipid Res. 34*, 317−324.
15. Forte, T. M., Bielicki, J. K., Goth-Goldstein, R., Selmek, J., and McCall, M. R. (1995) Recruitment of cell phospholipids and cholesterol by apolipoproteins A-II and A-I: formation of nascent apolipoprotein-specific HDL that differ in size, phospholipid composition, and reactivity with LCAT, *J. Lipid Res. 36*, 148−157.
16. Fielding, C. J., and Fielding, P. E. (1995) Molecular physiology of reverse cholesterol transport, *J. Lipid Res. 36*, 211−228.
17. Castro, G. R., and Fielding, C. J. (1988) Early incorporation of cell-derived cholesterol into pre-beta-migrating high-density lipoprotein, *Biochemistry 27*, 25−29.
18. Vaughan, A. M., and Oram, J. F. (2003) ABCA1 redistributes membrane cholesterol independent of apolipoprotein interactions, *J. Lipid Res. 44*, 1373−1380.
19. Panagotopulos, S. E., Witting, S. R., Horace, E. M., Hui, D. Y., Maiorano, J. N., and Davidson, W. S. (2002) The role of apolipoprotein A-I helix 10 in apolipoprotein-mediated cholesterol efflux via the ATP-binding cassette transporter ABCA1, *J. Biol. Chem. 277*, 39477−39484.
20. Fitzgerald, M. L., Morris, A. L., Rhee, J. S., Andersson, L. P., Mendez, A. J., and Freeman, M. W. (2002) Naturally Occurring Mutations in the Largest Extracellular Loops of ABCA1 Can Disrupt Its Direct Interaction with Apolipoprotein A-I, *J. Biol. Chem. 277*, 33178−33187.
21. Chroni, A., Liu, T., Gorshkova, I., Kan, H. Y., Uehara, Y., von Eckardstein, A., and Zannis, V. I. (2003) The Central Helices of ApoA-I Can Promote ATP-binding Cassette Transporter A1 (ABCA1)-mediated Lipid Efflux. Amino Acid Residues 220−231 of the Wild-Type ApoA-I are Required for Lipid Efflux in vitro and High-Density Lipoprotein Formation in vivo, *J. Biol. Chem. 278*, 6719−6730.
22. Gorshkova, I. N., Liu, T., Zannis, V. I., and Atkinson, D. (2002) Lipid-free structure and stability of apolipoprotein A-I: Probing the central region by mutation, *Biochemistry 41*, 10529−10539.
23. Liadaki, K. N., Liu, T., Xu, S., Ishida, B. Y., Duchateaux, P. N., Krieger, J. P., Kane, J., Krieger, M., and Zannis, V. I. (2000) Binding of High-Density Lipoprotein (HDL) and Discoidal Reconstituted HDL to the HDL Receptor Scavenger Receptor Class B Type I. Effect of Lipid Association and ApoA-I Mutations on Receptor Binding, *J. Biol. Chem. 275*, 21262−21271.
24. Liu, T., Krieger, M., Kan, H. Y., and Zannis, V. I. (2002) The Effects of Mutations in Helices 4 and 6 of ApoA-I on Scavenger Receptor Class B Type I (SR-BI)-mediated Cholesterol Efflux Suggest That Formation of a Productive Complex between Reconstituted High-Density Lipoprotein and SR-BI Is Required for Efficient Lipid Transport, *J. Biol. Chem. 277*, 21576−21584.
25. Luckow, V. A., Lee, S. C., Barry, G. F., and Olins, P. O. (1993) Efficient Generation of Infectious Recombinant Baculoviruses by Site-Specific Transposon-Mediated Insertion of Foreign Genes Into A Baculovirus Genome Propagated in Escherichia-Coli, *J. Virol. 67*, 4566−4579.
26. Anderson, D., Harris, R., Polayes, D., Ciccarone, V., Donahue, R., Gerard, G., Haces, A., Whitford, W., Bloom, F., Luckow, V.,

and Jessee, J. (1995) Rapid Generation of Recombinant Baculovirus and Expression of Foreign Genes Using the Bac-To-Bac-(Tm) Expression System, *FASEB J. 9*, A1464.
27. Sorci-Thomas, M. G., Parks, J. S., Kearns, M. W., Pate, G. N., Zhang, C., and Thomas, M. J. (1996) High level secretion of wild-type and mutant forms of human proapoA-I using baculovirus-mediated Sf-9 cell expression, *J. Lipid Res. 37*, 673−683.
28. Crowe, J., Masone, B. S., and Ribbe, J. (1995) One-step purification of recombinant proteins with the 6xHis tag and Ni-NTA resin, *Mol. Biotechnol. 4*, 247−258.
29. Crowe, J., Masone, B. S., and Ribbe, J. (1996) One-step purification of recombinant proteins with the 6xHis tag and Ni-NTA resin, *Methods Mol. Biol. 58*, 491−510.
30. Gorshkova, I. N., Liadaki, K., Gursky, O., Atkinson, D., and Zannis, V. I. (2000) Probing the lipid-free structure and stability of apolipoprotein A-I by mutation, *Biochemistry 39*, 15910−15919.
31. Reardon, C. A., Kan, H. Y., Cabana, V., Blachowicz, L., Lukens, J. R., Wu, Q. Z., Liadaki, K., Getz, G. S., and Zannis, V. I. (2001) In vivo studies of HDL assembly and metabolism using adenovirus-mediated transfer of apoA-I mutants in apoA-I-deficient mice, *Biochemistry 40*, 13670−13680.
32. Laccotripe, M., Makrides, S. C., Jonas, A., and Zannis, V. I. (1997) The carboxyl-terminal hydrophobic residues of apolipoprotein A-I affect its rate of phospholipid binding and its association with high-density lipoprotein, *J. Biol. Chem. 272*, 17511−17522.
33. Markwell, M. A. (1982) A new solid-state reagent to iodinate proteins. I. Conditions for the efficient labeling of antiserum, *Anal. Biochem. 125*, 427−432.
34. Li, X. P., Kan, H. Y., Lavrentiadou, S., Krieger, M., and Zannis, V. (2002) Reconstituted discoidal ApoE-phospholipid particles are ligands for the scavenger receptor BI−The amino-terminal 1−165 domain of ApoE suffices for receptor binding, *J. Biol. Chem. 277*, 21149−21157.
35. Fitzgerald, M. L., Mendez, A. J., Moore, K. J., Andersson, L. P., Panjeton, H. A., and Freeman, M. W. (2001) ATP-binding Cassette Transporter A1 Contains an NH2-terminal Signal Anchor Sequence That Translocates the Protein's First Hydrophilic Domain to the Exoplasmic Space, *J. Biol. Chem. 276*, 15137−15145.
36. Bligh, E. G., and Dyer, W. J. (1959) *Can. J. Biochem. Physiol. 37*, 911−918.
37. Nolte, R. T., and Atkinson, D. (1992) Conformational analysis of apolipoprotein A-I and E-3 based on primary sequence and circular dichroism, *Biophys. J. 63*, 1221−1239.
38. Borhani, D. W., Rogers, D. P., Engler, J. A., and Brouillette, C. G. (1997) Crystal structure of truncated human apolipoprotein A-I suggests a lipid-bound conformation, *Proc. Natl. Acad. Sci. U.S.A. 94*, 12291−12296.
39. Miccoli, R., Zhu, Y., Daum, U., Wessling, J., Huang, Y., Navalesi, R., Assmann, G., and von Eckardstein, A. (1997) A natural apolipoprotein A-I variant, apoA-I (L141R)Pisa, interferes with the formation of alpha-high-density lipoproteins (HDL) but not with the formation of pre beta 1-HDL and influences efflux of cholesterol into plasma, *J. Lipid Res. 38*, 1242−1253.
40. Miccoli, R., Bertolotto, A., Navalesi, R., Odoguardi, L., Boni, A., Wessling, J., Funke, H., Wiebusch, H., von Eckardstein, A., and Assmann, G. (1996) Compound Heterozygosity for a Structural Apolipoprotein A-I Variant, Apo A-I(L141R)Pisa, and an Apolipoprotein A-I Null Allele in Patients With Absence of HDL Cholesterol, Corneal Opacifications, and Coronary Heart Disease, *Circulation 94*, 1622−1628.
41. Lapicka-Bodzioch, K., Bodzioch, M., Krull, M., Kielar, D., Probst, M., Kiec, B., Andrikovics, H., Bottcher, A., Hubacek, J., Aslanidis, C., Suttorp, N., and Schmitz, G. (2001) Homogeneous assay based on 52 primer sets to scan for mutations of the ABCA1 gene and its application in genetic analysis of a new patient with familial high-density lipoprotein deficiency syndrome, *Biochim. Biophys. Acta 1537*, 42−48.
42. Matsunaga, T., Hiasa, Y., Yanagi, H., Maeda, T., Hattori, N., Yamakawa, K., Yamanouchi, Y., Tanaka, I., Obara, T., and Hamaguchi, H. (1991) Apolipoprotein A-I deficiency due to a codon 84 nonsense mutation of the apolipoprotein A-I gene, *Proc. Natl. Acad. Sci. U.S.A. 88*, 2793−2797.
43. McNeish, J., Aiello, R. J., Guyot, D., Turi, T., Gabel, C., Aldinger, C., Hoppe, K. L., Roach, M. L., Royer, L. J., de Wet, J., Broccardo, C., Chimini, G., and Francone, O. L. (2000) High-density lipoprotein deficiency and foam cell accumulation in mice with targeted disruption of ATP-binding cassette transporter-1, *Proc. Natl. Acad. Sci. U.S.A. 97*, 4245−4250.
44. Williamson, R., Lee, D., Hagaman, J., and Maeda, N. (1992) Marked reduction of high density lipoprotein cholesterol in mice genetically modified to lack apolipoprotein A-I, *Proc. Natl. Acad. Sci. U.S.A. 89*, 7134−7138.
45. Wang, N., Silver, D. L., Costet, P., and Tall, A. R. (2000) Specific binding of ApoA-I, enhanced cholesterol efflux, and altered plasma membrane morphology in cells expressing ABC1, *J. Biol. Chem. 275*, 33053−33058.
46. Wilson, C., Wardell, M. R., Weisgraber, K. H., Mahley, R. W., and Agard, D. A. (1991) Three-dimensional structure of the LDL receptor-binding domain of human apolipoprotein E, *Science 252*, 1817−1822.
47. Remaley, A. T., Stonik, J. A., Demosky, S. J., Neufeld, E. B., Bocharov, A. V., Vishnyakova, T. G., Eggerman, T. L., Patterson, A. P., Duverger, N. J., Santamarina-Fojo, S., and Brewer, H. B., Jr. (2001) Apolipoprotein specificity for lipid efflux by the human ABCAI transporter, *Biochem. Biophys. Res. Commun. 280*, 818−823.
48. Remaley, A. T., Thomas, F., Stonik, J. A., Demosky, S. J., Bark, S. E., Neufeld, E. B., Bocharov, A. V., Vishnyakova, T. G., Patterson, A. P., Eggerman, T. L., Santamarina-Fojo, S., and Brewer, H. B. (2003) Synthetic amphipathic helical peptides promote lipid efflux from cells by an ABCA1-dependent and an ABCA1-independent pathway, *J. Lipid Res. 44*, 828−836.
49. Fitzgerald, M. L., Morris, A. L., Chroni, A., Mendez, A. J., Zannis, V. I., and Freeman, M. W. (2003) ABCA1 and amphipathic apolipoproteins form high affinity molecular complexes required for cholesterol efflux, *J. Lipid Res.*, in press.
50. Borghini, I., Barja, F., Pometta, D., and James, R. W. (1995) Characterization of subpopulations of lipoprotein particles isolated from human cerebrospinal fluid, *Biochim. Biophys. Acta 1255*, 192−200.
51. Pitas, R. E., Boyles, J. K., Lee, S. H., Hui, D., and Weisgraber, K. H. (1987) Lipoproteins and their receptors in the central nervous system. Characterization of the lipoproteins in cerebrospinal fluid and identification of apolipoprotein B, E(LDL) receptors in the brain, *J. Biol. Chem. 262*, 14352−14360.
52. Huang, Y., von Eckardstein, A., Wu, S., Maeda, N., and Assmann, G. (1994) A plasma lipoprotein containing only apolipoprotein E and with gamma mobility on electrophoresis releases cholesterol from cells, *Proc. Natl. Acad. Sci. U.S.A. 91*, 1834−1838.
53. Boyles, J. K., Pitas, R. E., Wilson, E., Mahley, R. W., and Taylor, J. M. (1985) Apolipoprotein E associated with astrocytic glia of the central nervous system and with nonmyelinating glia of the peripheral nervous system, *J. Clin. Invest. 76*, 1501−1513.
54. Murakami, M., Ushio, Y., Morino, Y., Ohta, T., and Matsukado, Y. (1988) Immunohistochemical localization of apolipoprotein E in human glial neoplasms, *J. Clin. Invest. 82*, 177−188.
55. Zannis, V. I., Zanni, E. E., Makrides, S. C., Kardassis, D., and Aleshkov, S. (1998) Role of apolipoprotein E in Alzheimer's disease, in *NATO ASI Series, Life Sciences* (Catravas, J. D., Ed.) pp 179−209, Plenum Press, New York.
56. Petit-Turcotte, C., Stohl, S. M., Beffert, U., Cohn, J. S., Aumont, N., Tremblay, M., Dea, D., Yang, L., Poirier, J., and Shachter, N. S. (2001) Apolipoprotein C-I expression in the brain in Alzheimer's disease, *Neurobiol. Dis. 8*, 953−963.
57. Karathanasis, S. K., Salmon, E., Haddad, I. A., and Zannis, V. I. (1985) Nucleotide and corresponding amino acid sequences of human apoA-I, apoA-II, apoC-I, apoCII, apoCIII and apoE cDNA clones, in *Biochemistry and Biology of Plasma Proteins 11* (Scanu, A. M., and Spector, A. A., Eds.) pp 475−493, Marcel-Dekker, Inc., New York.

BI035813P